ID-1274

SPLIT ANGLE-PLY BEAM SPECIMEN FOR MEASUREMENT OF FRACTURE TOUGHNESS WITH MODE III STRESS STATE

Kunigal Shivakumar, Srikant Ghantae* and Matthew Sharpe
Center for Composite Materials Research
North Carolina A&T State University
Greensboro, NC 27411, USA
*Volvo Trucks North America, Greensboro, NC 27409
Phone (336) 334-7411 Ext. 2112 and Email: kunigal@ncat.edu

SUMMARY: A detailed three-dimensional non-linear contact stress analysis of split angle-ply beam specimen subjected to DCB and ENF type loading was performed. The beam was made up of +θ and -θ arms with a delamination in-between them. These angles represent an extreme segregation of stacking sequence and expect to produce large normal-shear and bending-twisting coupling. The analysis was conducted for different values of θ for unidirectional and woven fabric composites. The anticlastic bending makes the G distribution to be non-linear (bowed) along the delam front. The bending-twisting coupling causes G_{III} stress-state and it is proportional to D_{16}/D_{11}. The maximum $(G_{III}/G_{Tav})_{av}$ is about 12% for DCB and 15% for ENF for unidirectional composite and about 7% for woven composite laminates. In most laminates used in aerospace industries the percent of G_{III} will be less than the above values and it can be estimated from D_{16}/D_{11} of the sublaminate. Therefore, DCB and ENF fracture tests on split angle-ply woven fabric composites should demonstrate the effect of G_{III} stress-states on G_c and G_{IIc} respectively. The carbon/vinyl ester composite split beam specimen can be fabricated at room temperature and with no curing residual stress.

KEYWORDS: Fracture Toughness, Split angle-ply Beam, G_{III}, Vacuum Assisted Resin Transfer Molding

INTRODUCTION

High specific stiffness and strength, tailorability to required thermo-mechanical properties, and shapability into any complex shapes makes reinforced polymeric composites to be attractive to aircraft, automobiles, ships, sporting goods, and other structural applications. Primary building block in laminated composites is a ply. The required design parameters of a structural component are obtained by stacking several layers in different directions and curing them together. Mismatch of Poisson's ratios and/or modulus [1-3] between layers causes stress discontinuity across the interface. These discontinuities may become singular even in the absence of cracks and delaminations [1-2]. Various test specimens and test apparatus' were developed to measure the delamination fracture toughness of unidirectional laminates under mode-I, mode-II and their combination stress-states [4-7]. In real structures, delaminations occur between two differently oriented plies. Dissimilar ply orientation introduces mode III stress-state as well. Therefore the fracture toughness measured from the unidirectional specimens under mode I and II stress-states may not be adequate for design of multidirectional laminates. In other words, effect of mode III stress-state on the measured mode I and II fracture toughnesses must be included. Davidson et al [8,9] and Carlson et al [10] conducted experimental and analytical study on multidirectional laminates that are commonly used in aircraft applications to understand the mode mixity. These studies and the work of Shivakumar and his associates [11,12] lead to the conclusion that the anti-clastic bending expressed in terms of sublaminate Poisson's ratio or a nondimensional parameter $D_c=(D_{12}^2/(D_{11}D_{22}))$ has to be small to achieve self similar advancement of a initially straight delamination front; otherwise the delam front curves as it progresses. Salman and Shivakumar [13] and Ghantae and Shivakumar [14] conducted a

detailed 3-D stress analysis of split angle-ply (+θ/−θ) beam specimen subjected to DCB and ENF type loading. They examined variation of G_I, G_{II} and G_{III} with ply orientation (0 to 45 deg) of the beam. The results concluded that for all non-zero ply orientated split beam specimens all three fracture modes exists at the delam front. The magnitude of G_{III} varies with ply-angle and reaching maximum value at θ=45 deg. Manufacturing of split angle-ply beam specimens for aerospace grade matrix system is impossible because of the curing stresses introduced during the cooling cycle of the high temperature cure resins. Therefore, split angle-ply beam specimens can not be fabricated.

Vinyl ester resin and its derivatives are chosen materials for applications like automobile, ship and civil infrastructure applications. These resins cure at room temperature. Vacuum Assisted Resin Transfer Molding (VARTM) is an accepted method for manufacturing large size and near net shape components. Advantages of this process are that it uses vacuum pressure, room temperature and no limitation on size of the component. The temperature rise during the processing was found to be less than 2^o F. Therefore, VARTM is an ideal process to manufacture split angle-ply beam specimen with no cure stresses and to evaluate the effect of G_{III} stress-state on the measured fracture toughnesses of laminates. The data generated should be applicable to composite structures made up of VARTM process and also provide qualitative guidelines for other aerospace composites. The objective of this paper is to summarize the results of references 13 and 14, present results for woven composite split angle-ply beam specimen, and then propose a test specimen for measuring the mode I and mode II fracture toughnesses in the presence of G_{III} stress-state.

SPLIT ANGLE-PLY BEAM SPECIMEN

Specimen Configuration

The split angle-ply beam specimen is made up of two layers of composite material with the top layer oriented at +θ and the bottom layer at −θ to the x-axis. The delamination is between +θ and −θ layers. The specimen configuration and coordinate system x, y and z, are shown in Fig 1. The beam is loaded in either opening (mode I) or sliding (mode II) mode, the stress-state at the delamination front will be a combination of mode-I, II, and III. Magnitude of these modes depends on the ply orientation. If θ=0 the stress-state is pure mode I for DCB and mode II for ENF type loading. The normal-shear and bending-twisting [15] coupling in angle-ply beams create G_{III} stress-states. The geometric parameters of the beam are length 'L', total thickness '2h' (each arm thickness is 'h'), width 'B' and the delamination of length 'a'. Values of L, B, h and a were 4-in, 1-in, 0.06-in, and 1-in, respectively.

Material System

The material chosen is a carbon woven fabric and vinyl ester resin composite with weave direction representing the principal material axis and the angle between this and the x is θ. The properties of this material and T300/5208 composite are given in Table 1. The subscripts refer to the principal directions of the material. Coefficients of A, B, and D matrices can be calculated using the classical laminate theory [15]. For the present study, the top and bottom arms are made of same material but have opposite fiber orientation. Therefore for each arm B_{ij}=0 (about the delam plane B_{ij} 0) and all elements of A_{ij} and D_{ij} are equal for top and bottom arms of the beam except $(A_{16})_\theta = -(A_{16})_{-\theta}$, $(A_{26})_\theta = -(A_{26})_{-\theta}$, $(D_{16})_\theta = -(D_{16})_{-\theta}$, $(D_{26})_\theta = -(D_{26})_{-\theta}$. These terms are associated with normal-shear and bending-twisting coupling. These coupling terms contribute to mode III singularity (τ_{zy}). At the free edge (z=0 and y=±b/2) shear stress τ_{zy} must become zero, this leads to development of mode II stress-state in DCB specimen and mode I stress-state in ENF specimen to satisfy the equilibrium condition [13,14]. Therefore, whatever the type of loading (DCB or ENF) on the split angle-ply beam laminate, the delamination front experiences all three modes of fracture.

Bending-Twisting and Anticlastic coupling parameters

Figure 2 shows the variation of D_{16}/D_{11} and D_c with ply orientation for T300/5208 unidirectional and carbon/vinyl ester woven composites. For the problem considered here these two distributions will be identical to those of Q_{16}/Q_{11} and $Q_{12}^2/(Q_{11}Q_{22})$. The D_{16}/D_{11} distribution is skewed with the maximum at θ=50 for unidirectional laminate, while it is at θ=22.5 for woven composite. This difference in distribution is due to differences in the degree of orthotropy of the two materials. For unidirectional laminates the D_{16} is maximum at θ=30, because of variation of D_{11} and θ, the maximum value of D_{16}/D_{11} occurred at θ=50 deg.

The D_c (or the effective Poisson's ratio) distribution is symmetric about θ=45 deg for both laminates. However the shape and peak values differed. Maximum anticlastic bending occurs at θ=45 deg for all orthotropic laminates.

FINITE ELEMENT ANALYSES

The split angle-ply beam specimens shown in fig. 1 are symmetric in geometry and loading about the delamination (z=0 plane) and y=0 planes. But materially, they are anti-symmetric. Therefore, full specimen was modeled to capture the asymmetric deformation and stresses. A commercial finite element code ANSYS version 5.5 was used throughout this study. Eight-node brick elements (SOLID46) were used to model the specimen. The element had twenty-four degrees of freedom and is capable of modeling isotropic as well as anisotropic materials. Several finite element idealizations were used in this study. A typical idealization is shown in Fig 3. This model had four equal divisions through the thickness of each of the delaminated arm. Thirty unequal divisions through the width, and a fine grading from crack front to the two ends of the specimen. The element length in front and back of the delam front was 0.003a (0.3% of the crack length).

Because, the delaminated surfaces are expected to contact with each other due to anticlastic bending or loading, surface to surface contact elements were used between the expected areas of contact. The analysis iteratively establishes the precise contact between the surfaces. Whenever a contact occurs, a stiff spring is introduced between the two surfaces and when they separate the spring stiffness was reduced to a very low value. This operation is automatically performed by the code by iteratively establishing the contact surface.

Four types of width refinements were used, namely, 10-equal, 10-, 20- and 30-graded divisions of the width. In the graded mesh case, the elements were finer towards the two free edges and coarser in the middle to capture the high stress gradient near the free edges. Details of boundary conditions, convergence study, and why this split laminate has no interfacial oscillatory singular stresses are in [14,15]. This paper presents a summary of split beam unidirectional and woven fabric composites.

Energy release rates were calculated using the three-dimensional virtual-crack-closure technique [12,17]. The delamination front was divided into segments same as the width refinement. At each segment G_T, G_I, G_{II}, and G_{III} were calculated by resolving the displacements behind and the forces at the delamination front in local coordinates of the front. The average values (G_{Tav}, G_{Iav}, G_{IIav} and G_{IIIav}) were calculated by numerically integrating over the delam front and dividing by the beam width.

RESULTS AND DISCUSSION

Finite element analysis of split angle-ply beam specimen was conducted for opening (DCB) and sliding (ENF) type loading. These two beams represent the two distinct loading types. Two materials namely, T300/3208 unidirectional and carbon/vinyl ester woven composites were used. The analysis was conducted for fiber orientations ranged from 0 to 90 deg for unidirectional composites and 0 to 45 deg for woven fabric composites. Distribution of energy release rates along the delam front and their averages for various cases mentioned above are presented.

Unidirectional Composites

Detailed distribution of G_I, G_{II} and G_{III} and G_T along the delam front for different ply orientation are presented in [13] for DCB loading and in [14] for ENF loading. Here, only a summary of the results is presented. Figure 4 shows the distribution of total energy release rate (G_T) along the delam front. For the range of angles considered G_T is nearly constant over the middle 75% length of the delamination front. Then G_T drops towards the two free edges and at the free edge it spikes to a large value. This jump phenomenon may be due to the free edge effect as explained in [18]. The G_I distribution was similar to G_T. The G_{II} was zero in the middle 75% length of the delam front and then rises to a large value at the free boundary. On the other hand, G_{III} is nearly constant over the middle 60% of the width of the beam and then it drops to nearly zero before rising to a large value at the free boundary.

Figure 5 shows the variation of average values of the three modes of energy release rates with ply orientation (θ). All three modes will reach extreme values at θ=40 deg, G_{av}, G_{IIav} and G_{IIIav} were 0.8, 0.09 and 0.12 times of G_{Tav} respectively. Notice also that G_{III} distribution is not symmetric as in the case of D_{16}/D_{11} distribution, discussed previously. The G_{III} increases with increase D_{16}/D_{11}. Both G_{III} and D_{16} are zero at θ=0 and 90.

The ENF loading had the similar results. The maximum $(G_{III}/G_T)_{av}$ was about 15% and it occurred at θ = 45.

Woven Fabric Composites

DCB Loading

Figure 6 shows distribution of normalized G_T along the delam front for five different (0, 15, 22.5, 30 and 45) ply orientations. Results of θ=0 has the lowest anticlastic bending effect, while θ=45 deg had the highest. The G curves varied from nearly flat for θ=0 to the largest bend for θ=45 deg. All other results fell in between these two sets. These shapes reflect how the crack front change as it propagates from the initial straight front. The G_I distribution (Fig 7) is almost similar to G_T distribution.

Figure 8 shows the distribution of normalized G_{II} along the delam front for θ=15, 22.5 and 30. G_{III} is zero for θ=0 and 45 deg. The G_{III} at the mid length of the delam is large and it becomes nearly zero near the free edge before it spikes at the free edge. The G_{III} is largest for θ=22.5 compared to all other angles. This trend agrees with distribution of D_{16}/D_{11} with θ (Fig 2). Variations of average values of GI, GII and GIII with ply orientation are shown in Fig 9. Comparing the figures 2 and 9, we can conclude that D_{16}/D_{11} is directly proportional to $(G_{III}/G_T)_{av}$. The largest value of G_{III} is about 7% of G_{Tav}.

ENF Loading

Figure 10 shows the variation of normalized G_T along the delam front for ply orientations of θ=0, 15, 22.5,30 and 45 deg. The G_T distribution is flat for θ=0 because of very low Poisson's ratio or D_c. Again the edge effect makes the G-curves to spike at the free edge. The variation of three modes of energy release rates with ply orientation is shown in fig 11. Both G_I and G_{III} peak at θ=22.5. These values were 5% and 6.5% of the G_{Tav}, respectively. The G_{III} variation is proportional to D_{16}/D_{11}.

CONCLUDING REMARKS

A detailed three-dimensional non-linear contact stress analysis of split angle-ply beam specimen subjected to DCB and ENF type loading was performed. The beam was made up of +θ and -θ arms with a delamination in-between them. These angles represent an extreme segregation of stacking sequence and expect to produce large normal-shear and bending-twisting coupling. The analysis was conducted for different values of θ for unidirectional and woven fabric composites. The anticlastic bending is due to the Poisson's ratio or D_c of the sublaminate. It is smallest for θ=0 and it was largest for θ=45 for both composites. The anticlastic bending makes the G distribution to be non-linear (bowed) along the delam front. The bending-twisting coupling causes G_{III} stress-state and its magnitude is nearly proportional to D_{16}/D_{11}. The average G_{III} is largest at θ=40 (12% of G_{Tav} for DCB and 15% for ENF) for

unidirectional composite and at θ=22.5 (7% of G_{Tav}) for woven composites laminate. The average G_{III} was slightly smaller for ENF loading (6.5%) compared to the DCB loaded specimen. In most laminates used in aerospace industries the percent of G_{III} will be less than that of 2-layer laminate and it can be estimated from D_{16}/D_{11} of the sublaminates. Therefore, DCB and ENF fracture tests on split angle-ply woven fabric composites should demonstrate the effect of G_{III} stress-states on G_{Ic} and G_{IIc} respectively. The carbon/vinyl ester composite split beam specimen can be fabricated at room temperature and with no curing residual stress.

ACKNOWLEDGEMENTS

Authors thank the Office of Naval Research for financial support through a grant N00014-99-0445. Dr. Yapa Rajapakse was the technical monitor of the grant. The second author also thanks Volvo Trucks Corp. for encouragement in conducting this research.

REFERENCES

1. Pipes, R.B. and Pagano, N.J., "Interlaminar Stresses in Composite Laminates under Uniform Axial Extension", *Journal of Composite Materials*, October 1970, pp. 538-548.
2. Raju, I. S. and Crews, J. H. Jr., " Interlaminar Stress Singularities at a Straight Free Edge in Composite Laminates", *J. Comput. Structure* 14, 1981, 21-28.
3. Salpekar, S.A., O' Brien, T.K. and Shivakumar, K.N., "Analysis of Local Delaminations Caused by Angle Ply Matrix Cracks", *J of Composite Materials*, 1996, Vol. 30 (4).
4. Russell, A.J. and Street K.N., "Factors Affecting the Interlaminar Fracture Energy of Graphite/Epoxy Laminate", *Progress in Science and Engineering of composites*, ed. T. Hayashi, K. Kawata and S. Umekawa. ICCM-IV, Tokyo, 1982, Pp. 279-286.
5. Russell, A. J., "On the Measurement of Mode II Interlaminar Fracture Energies". *DREP Materials Report* 82-0, December 1982.
6. Crews, J.H., Jr. and Reeder, J.R., "A Mixed Mode Bending Apparatus for Delamination Testing" , *NASA TM 100662*, Aug 1988.
7. Shivakumar, K.N., Crews, J.H. Jr., and Avva, V.S.,"Modified Mixed-Mode Fracture Test Apparatus for Measuring Interlaminar Fracture Toughness of Composite Laminates" *13th ASTM-Symposium on Composite Material : Testing and Design*, Orlando, Fl May 1996.
8. Davidson, B.D, Altonen, C.S. and Polaha, J.J., "Effect of stacking sequence on Delamination Toughness and Delamination Growth behavior in Composite ENF Specimens" *Twelfth Symposium on Composite Material: Testing & Design*, ed. C. R. Saff and R. Deo. ASTM STP 1274, 1996, pp. 393-413.
9. Davidson, B.D, Kruger, R. and Konig, M., "Three Dimensional Analysis and Resulting Design recommendations for Unidirectional and Multidirectional ENF Test" *J. Composite Material*, 29(16), 1995, pp. 2108-2133.
10. Ozdil, F., Carlsson, L.A. and Davies, P., " Beam analysis of Angle ply laminate for ENF Specimens" *Comp. Sci. ech*., 58, 1998.
11. Crews, J.H. Jr., Shivakumar, K.N. and Raju, I.S., "Strain Energy Release rate Distributions for DCB Specimens", *AIAA Journal*, Vol. 29, Oct 1991, pp. 1686-1691.
12. Raju, I.S., Shivakumar, K.N. and Crews J.H. Jr., "Three-Dimensional Static Analysis of a Composite DCB Specimen", *AIAA Journal* Vol. 26, Dec 1988, pp. 1493-1498.
13. Salman-Ul-Haq. and Shivakumar, K.N., "Three-Dimensional Analysis if Angle ply split beam specimens under opening mode loading", *Proceedings of ASC 14th technical conference*, 1999, pp 427-436.
14. Ghantae, S. and Shivakumar, K.N., "Three-Dimensional Analysis if Angle ply split beam specimens under ENF Type Loading", *Proceedings of ASC 15th technical conference*, 2000.
15. Jones, R. M., "Mechanics of Composite Materials". Hemisphere Publishing Corporation, New York, 1975,.

16. Davidson, B.D, Kruger, R. and Konig, M., "Effect of Stacking Sequence on Energy release rate distributions in Multidirectional DCB and ENF Specimens", *Engg, Fracture Mech*. Vol. 55 No. 4, 1996, pp. 931-938.
17. Shivakumar, K.N, Tan, P.W. and Newman, J. C. Jr., "A Virtual Crack-Closure Technique for Calculating Stress Intensity Factors for Cracked 3-D Bodies." *International Journal of Fracture*, 1988, Vol. 36 R43-R50.
18. Shivakumar, K.N. and Raju, I.S, "Treatment of singularities in cracked bodies" International journal of fracture, 1990, pp. 159-178

Table 1. Material properties

Properties	T300/5208 Carbon/Epoxy	Woven Carbon/Vinyl ester
E_{11}, Msi	19.00	8.530
E_{22}, Msi	1.89	8.530
E_{33}, Msi	1.89	0.995
G_{23}, Msi	0.70	0.458
G_{13}, Msi	0.93	0.458
G_{12}, Msi	0.93	0.468
ν_{23}	0.35	0.27
ν_{31}	0.34	0.27
ν_{12}	0.34	0.02

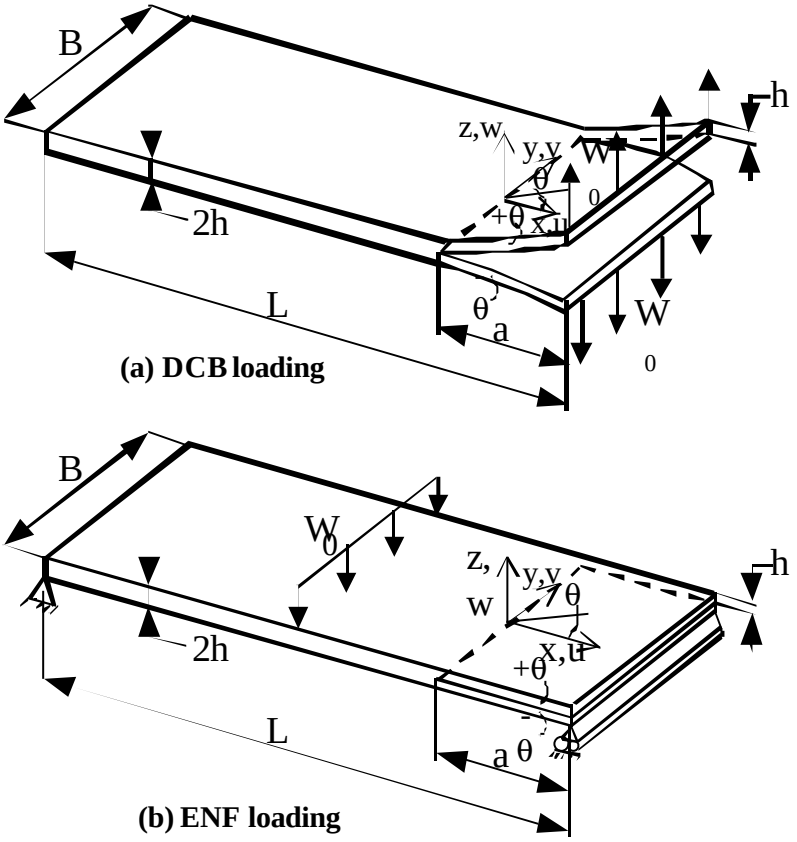

Fig. 1 Typical split beam specimen.

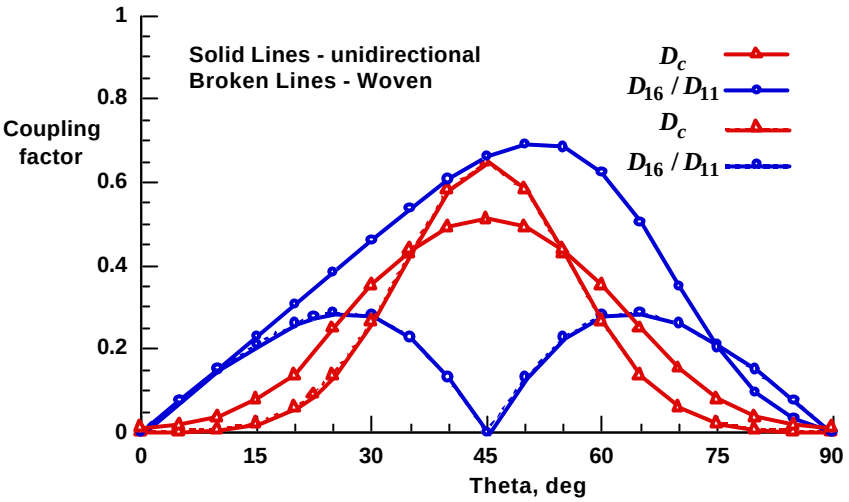

Fig. 2 Variation of coupling factors with ply orientation.

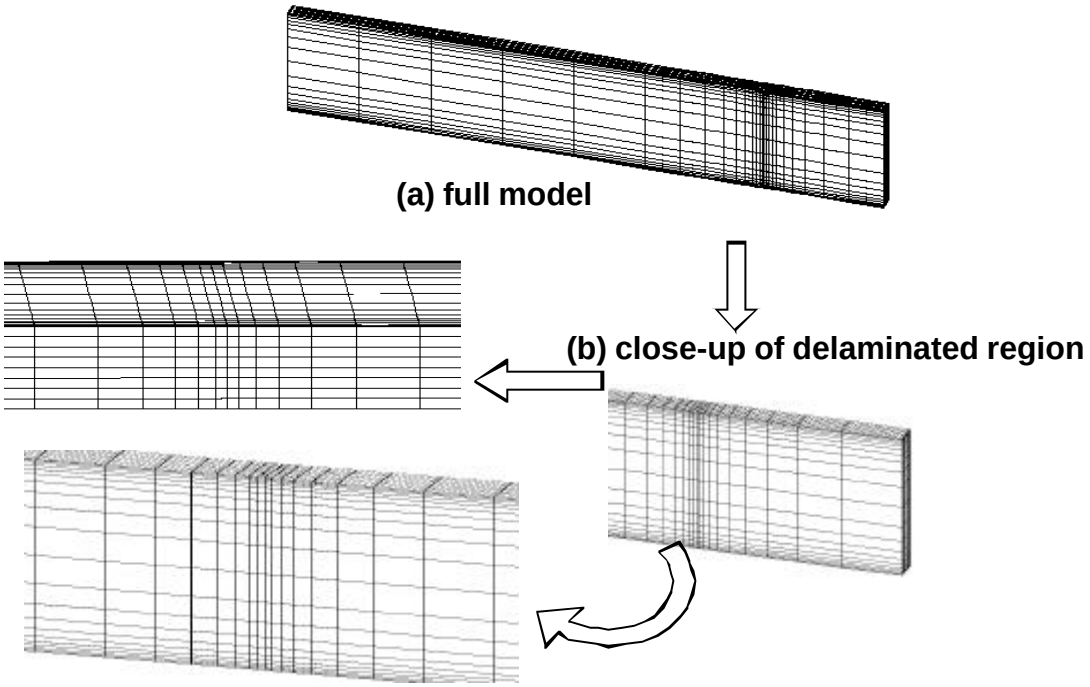

Fig. 3 Typical finite element idealization of the specimen.

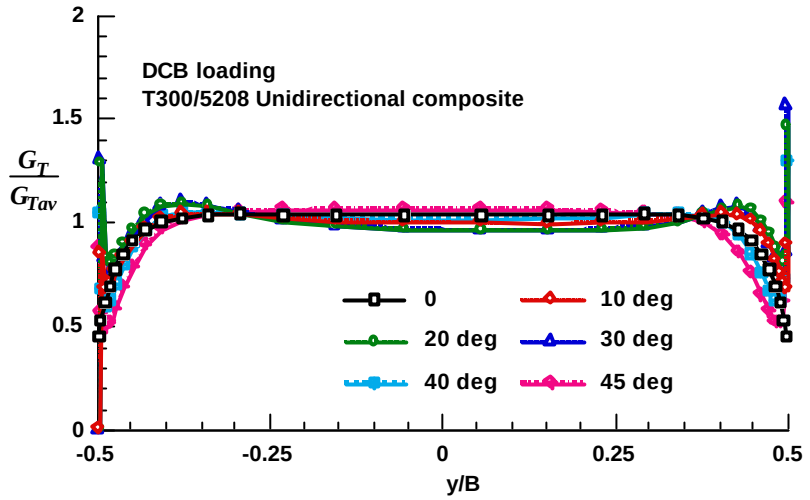

Fig. 4 Variation of normalized G_T along the delam front.

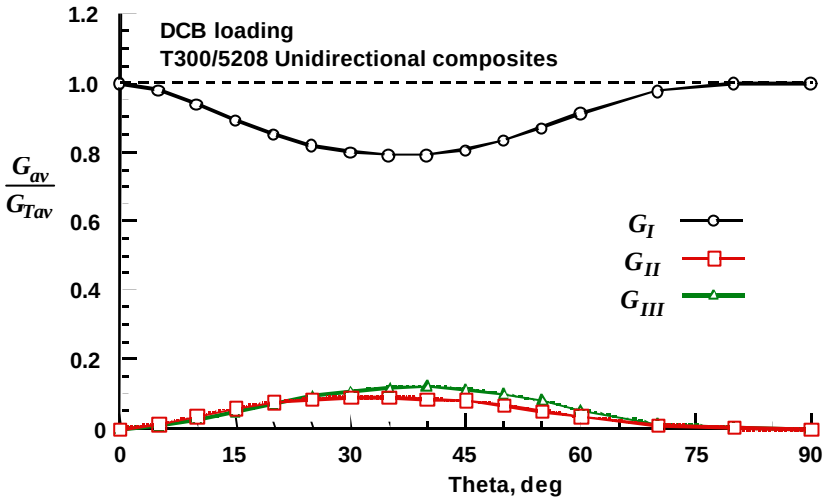

Fig. 5 Variation of normalized energy release rates with ply orientation.

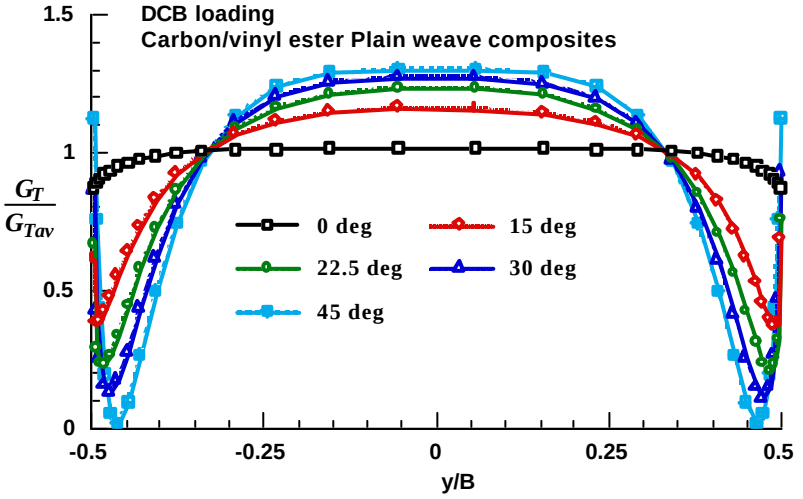

Fig. 6 Variation of normalized G_T along the delam front for woven fabric composites.

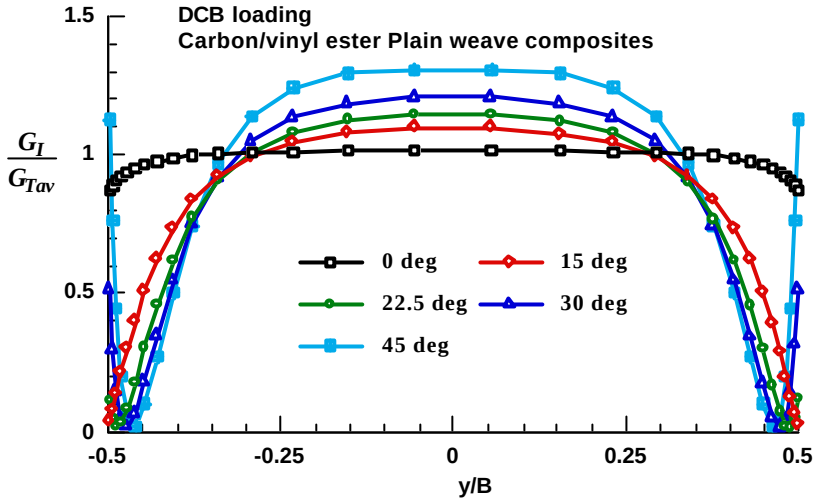

Fig. 7 Variation of normalized G_I along the delam front for woven fabric composites.

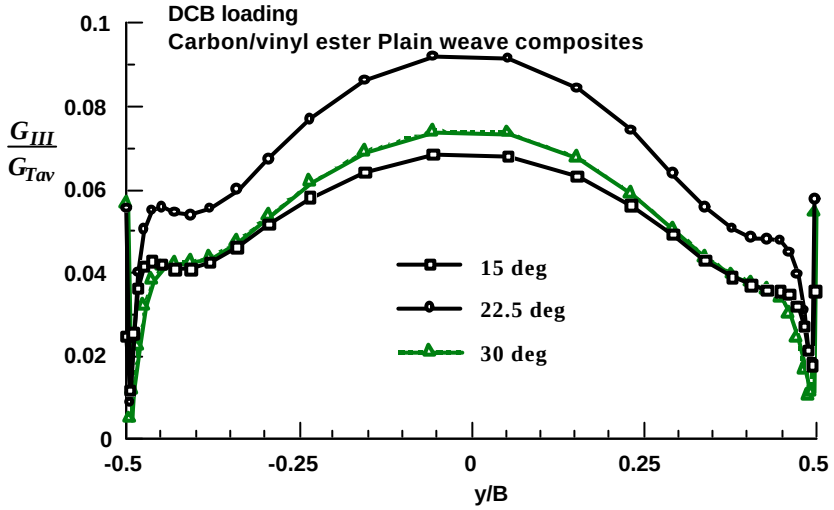

Fig. 8 Variation of normalized G_{III} along the delam front for woven fabric composites.

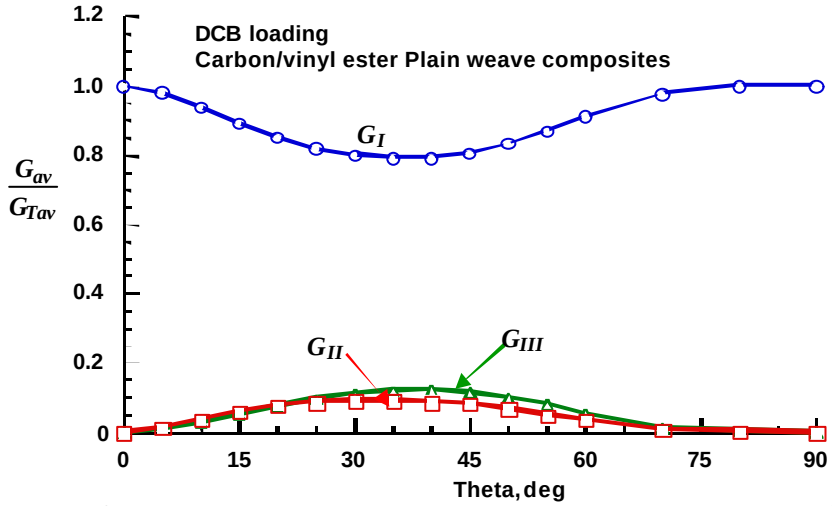

Fig. 9 Variation of normalized average energy release rates with ply orientation for woven fabric composites.

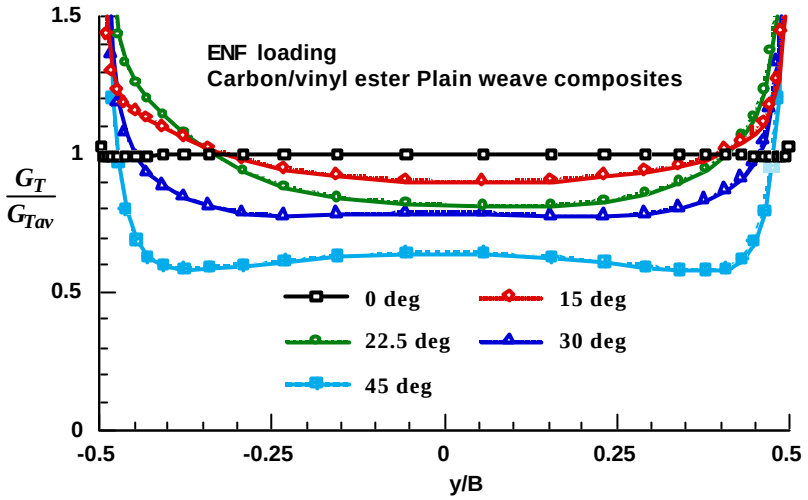

Fig. 6 Variation of normalized G_T along the delam front for woven fabric composites.

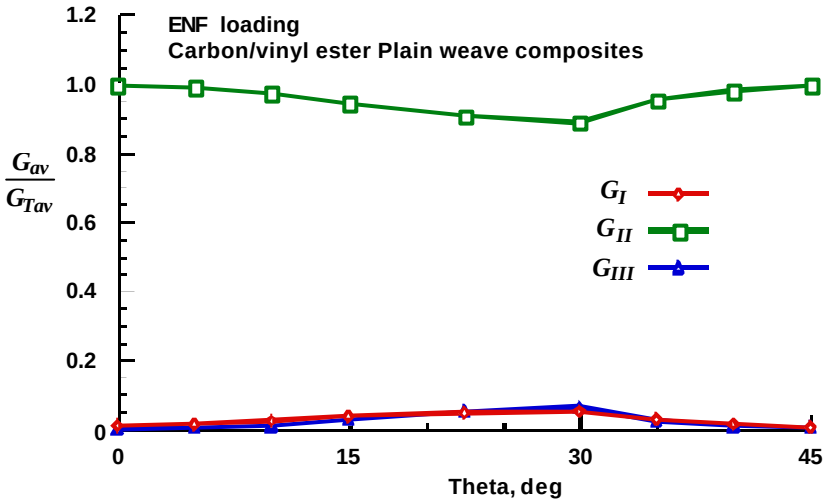

Fig. 11 Variation of normalized average energy release rates with ply orientation for woven fabric composites.